

Self-imaging effects in curved gradient index multimode interference structures made by K⁺–Na⁺ ion exchange

MAREK BŁAHUT*, DAWID FRONIEWSKI

Institute of Physics, Silesian University of Technology, Bolesława Krzywoustego 2,
44-100 Gliwice, Poland

*Corresponding author: marek.blahut@polsl.pl

The paper presents an analysis of self-imaging phenomena in gradient multimode interference (MMI) structures produced by K⁺–Na⁺ ion exchange in glass. This investigation concerned curved MMI structures with various geometries – for the linear, concave function described by an exponential function, and the convex structure connected with a cosine course. The relations derived characterizing the relative shortening of the length of propagation for N -fold images have been confirmed by numerical simulations using the beam propagation method (BPM) of symmetrically excited gradient splitters 1×2.

Keywords: multimode interference structures, ion-exchange.

1. Introduction

For a score of years an intensive development of investigations has been observed concerning the technology of elements of integrated optics, making use of interference effects occurring in a multimode waveguide. The effect of intermode interference is the so-called self-imaging of the input field exciting the multimode section, as a result of which the input field is reproduced at specified distances as simple, mirrored and multiplied images [1, 2]. This phenomenon constitutes a basis for the operation of multimode interference (MMI) structures. The application of the technology based on MMI, which permits a considerable miniaturization of the input and output elements of the optics system as well as those of coupling and splitting the optical signal, provides new possibilities of developing integrated optics system and waveguide sensors [1–3].

Gradient structures made by ion exchange in glass are attractive for MMI technology. Ion exchange technique making use of multi-step diffusion processes, electrodiffusion, heating, diffusive and electrodiffusive burying makes it possible to easily change the modal properties of the waveguides obtained on which the intermode interference effects depend.

In [4–8] it has been affirmed that self-imaging effects can occur in gradient waveguides produced by $K^+ - Na^+$ and $Ag^+ - Na^+$ ion exchange method and their applications, among others, in the technology of splitters 1×2 have been presented. Dimensions of such structures depend mainly on the length of a straight multimode waveguide constituting the interference section. Any change of the shape of this element may lead to the shortening of the way of self-imaging and greater miniaturization of the MMI elements, as has been proved by investigations of step-index waveguides [9–12].

The aim of the present paper is to demonstrate the influence of the shape of the gradient MMI section on the geometry and operating characteristics of splitters $1 \times N$ obtained by $K^+ - Na^+$ ion exchange. Numerical simulations were carried out by applying the beam propagation method (BPM). Making use of the effective index method it has been proved that there exists a connection between the gradient MMI structures and the equivalent step-index structures. Subsequently, equations have been derived which permit estimation of the effect of shortening the length of propagation for N -fold images for selected geometries of gradient index MMI sections.

2. Operating principles of MMI structures

As far as the behavior of MMI structures with a varying geometry is concerned, it is essential to recall the fundamental properties of straight structures. It consists of a group of monomode waveguides, which define the input field, of the wide multimode section where the interference effects of modal fields are observed, and output monomode waveguides. Figure 1 presents an example of the symmetrical coupler/splitter 1×2 .

In most cases the MMI structures are single-mode in the y direction. In such a case, the width and length of the waveguide exceed considerably its depth, and thus it is to be assumed that the modes behave similarly, independently of the depth y . This leads to the analysis of this problem based on its two-dimensional representation [2].

The phenomena of self-imaging in the MMI structures are well known for step-index waveguides [1, 2]. They result from the quadratic dependence of the propagation constants characterizing these waveguides on the number of the mode. In the case of multimode waveguide of the width W_0 it may be expressed by the formula:

$$\beta_l \approx k_0 n_C - \frac{(l + 1)^2 \pi \lambda_0}{4 n_C W_{e0}^2} \quad (1)$$

where $k_0 = 2\pi/\lambda_0$ is the wave number in a vacuum, n_C is the refractive index of the core, l denotes the number of mode, and W_{e0} is the effective width of the waveguide, characterizing the depth penetration of the field to the surroundings. In waveguides of a large difference between refractive indices of the core and surroundings the depth of penetration is very small, so that we may assume that $W_{e0} \approx W_0$.

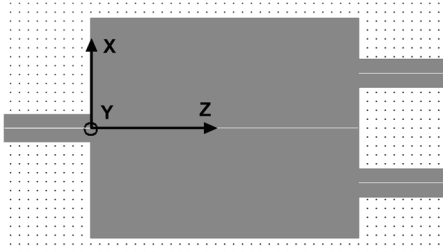


Fig. 1. Diagram of MMI structure for the coupler/splitter 1×2 configuration.

On the basis of Eq. (1) it can be shown [1] that the N -fold image of the input field for any arbitrary position of the input field is formed at the distance L_N^0 satisfying the condition:

$$L_N^0 = \frac{n}{N} \frac{4n_C W_{e0}^2}{\lambda_0}, \quad n = 1, 2, \dots \quad (2)$$

In the case of the symmetrical excitation presented in Fig. 1, when merely even modes are excited, this distance is shortened four times:

$$L_N^0 = \frac{n}{N} \frac{n_C W_{e0}^2}{\lambda_0}, \quad n = 1, 2, \dots \quad (3)$$

A similar quadratic dependence of propagation length for N -fold images on the width of the MMI section occurs in gradient waveguides obtained by the exchange of K^+ – Na^+ ions [5], which allows the properties of gradient MMI structures and the properties of step-index structures to be related. Figure 2 illustrates the distribution of the refractive index $n(x, y)$ of the gradient MMI section achieved by means of a numerical solution of the non-linear equation of diffusion through the window of 50 μm in width, characterizing the K^+ – Na^+ ion exchange [7] into glass BK-7:

$$\frac{\partial C_K}{\partial t} = \nabla \left[\frac{D_K}{1 - (1 - m)C_K} \nabla C_K \right] \quad (4)$$

where C_K is the dopant K^+ ions concentration, proportional to the refractive index change. Material parameters of the technological process – self-diffusion coefficient

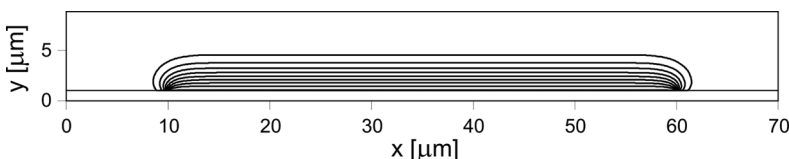


Fig. 2. Distribution of the refractive index in a gradient waveguide for the K^+ – Na^+ ion exchange through the window $W_0 = 50 \mu m$.

of K^+ ions $D_K = 2.18 \mu\text{m}^2/\text{h}$, the mobility ratio of the ions K^+ and Na^+ $\mu = 0.9$, and the maximum of the refractive index change $\Delta n = 0.095$ were determined by measuring the respective planar index profiles using inverse Wenzel–Kramers–Brillouin (IWKB) method.

For the diffusion time $t = 1 \text{ h}$ the waveguide is for the wavelength $\lambda_0 = 0.633 \mu\text{m}$ a single-mode in the y direction perpendicular to the surface of the substrate. It guides 13 modes in the x direction. The distribution of the refractive index for the depth y does not change in the transverse direction x . It is to be expected that the corresponding one-dimensional profile calculated by means of the effective refractive index method would approximate the distribution of the step-index.

Figure 3 presents profiles of the effective refractive indices calculated numerically based on two-dimensional distribution concerning the $K^+–\text{Na}^+$ ion exchange through the windows of 40, 50 and 60 μm in width. The distributions achieved approximate the distribution of the step-index. Note that in the case of the assumed range of changes in the window widths the value of the effective index does not change with the width of the MMI section, amounting to $n_{\text{eff}} = 1.5163$. Assuming that their mode characteristics comply with Eq. (1), we present in Fig. 4 the dependence of the numerically calculated propagation constants on the expression $(l + 1)^2/W_0^2$, concerning various widths of diffusion windows and the number of modes. This dependence is described with a good approximation by a straight line. The inclination of the straight line determines the mean value of the effective waveguide width for all the modes $W_{e0} \approx 1.02 W_0$.

In order to assess the efficiency of approximation of self-imaging phenomena in the gradient diffusive waveguides, based on equivalent characteristics of step-index waveguides, the position of N -fold images could be determined for various widths of the diffusion windows in the symmetrically excited gradient MMI structures, making

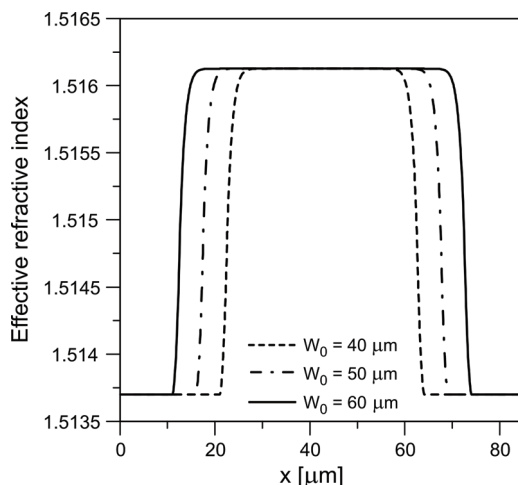


Fig. 3. Effective refractive indices of gradient waveguides obtained by diffusion through windows of 40, 50 and 60 μm .

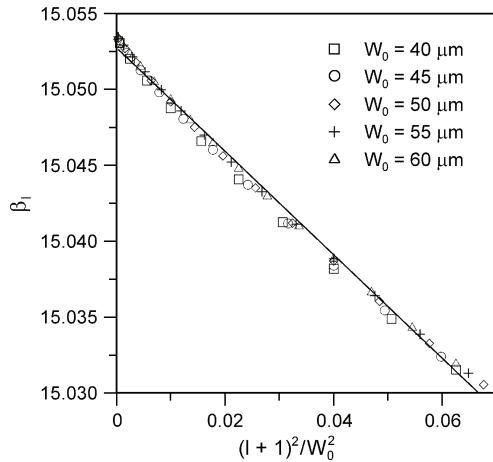


Fig. 4. Dependence of the propagation constants of gradient waveguides on the number of the mode and the width of the window of diffusion.

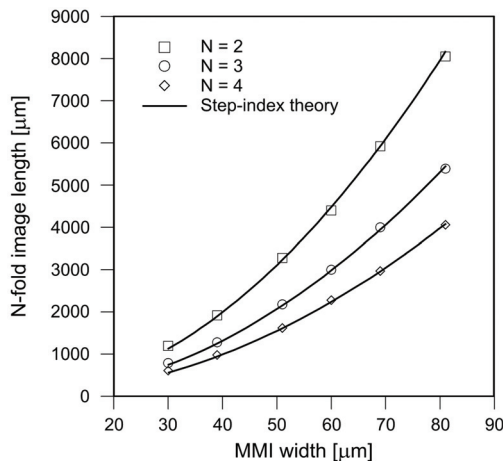


Fig. 5. Position of N -fold images in symmetrically excited gradient MMI structure.

use of the BPM method. In Figure 5, the results of these calculations have been compared with the characteristics determined from relation (3) for $W_{e0} \approx 1.02 \times W_0$. Note a considerable compliance of the results obtained, which allows the values of the propagation lengths to be assessed for N -fold images in gradient curved MMI structures based on the relations characterizing the step-index waveguides.

3. Phenomena of self-imaging in curved MMI structures

The description of the self-imaging effect in curved MMI structures must take into account the dependence of the relative differences of the phases between the modes

on the shape of the curves. If the change of the width of MMI section with its length is a slowly varying function, no effects of mode coupling ought to be observed. Under such conditions the phenomena of the mode fields interference may be analyzed within the theory of local modes. In each step of propagation in the MMI section a set of propagation constants $\beta_l(z)$ is formed, connected with the local effective width $W_e(z)$ of the section. Therefore, the difference of phases between the fundamental mode and the l -th mode on the length of propagation L may be expressed by the equation [9]:

$$\Delta\varphi = \int_0^L (\beta_0 - \beta_l) dz \quad (5)$$

Applying formula (1) we get:

$$\Delta\varphi = \frac{l(l+2)\pi\lambda_0}{4n_{\text{eff}}} \int_0^L \frac{1}{W_e^2(z/L)} dz \quad (6)$$

where n_{eff} is the effective refractive index of gradient multimode waveguide. The varying width of the MMI section is expressed by the function of the relative changes of the propagation length.

Substituting $t = z/L$ and relating the width of curved MMI section to the width of straight section W_{e0} we get the following equation:

$$\Delta\varphi = \frac{l(l+2)\pi\lambda_0}{4n_{\text{eff}} W_{e0}^2} L \int_0^1 \frac{W_{e0}^2}{W_e^2(t)} dt \quad (7)$$

The formation of N -fold images is conditioned by the phase coincidence of the interfering modes. When the length of MMI section corresponds to the propagation length L_N for N -fold images, the following condition should be satisfied [11]:

$$\Delta\varphi = l(l+2) \frac{n}{N} \pi, \quad n = 1, 2, \dots \quad (8)$$

Comparing (8) with (7) we get for $n = 1$ equation determining the length of propagation for N -fold images in curved MMI section:

$$L_N = \frac{4n_{\text{eff}} W_{e0}^2}{\lambda_0 N} \left/ \int_0^1 \frac{W_{e0}^2}{W_e^2(t)} dt \right. = L_N^0 \left/ \int_0^1 \frac{W_{e0}^2}{W_e^2(t)} dt \right. \quad (9)$$

where L_N^0 is the propagation length for N -fold images in straight MMI section, as described by Eq. (2). If the surface area of the straight MMI section is larger than the surface area of the curved section, then according to Eq. (9) the propagation length

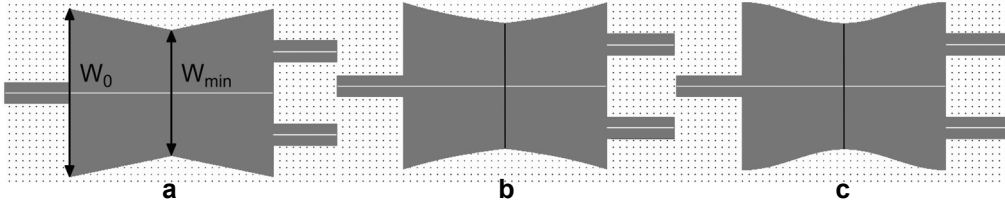


Fig. 6. Geometry of analyzed MMI structures.

L_N is shortened. Similar relations can be obtained in the case of a symmetrical excitation of the MMI structures with L_N^0 expressed by Eq. (3).

The phenomena of self-imaging have been analyzed in MMI structures the shapes of which can be seen in Fig. 6. The geometry of all the sections is symmetrical with respect to the axis of symmetry passing through the centre of the structure. The minimum value of the concentration W_{\min} of analyzed section amounted to 75% of the initial value W_0 , the reasons for which will be dealt with in Section 5. The change of the shape of the MMI structure is described by: *i*) the linear function, *ii*) exponential function (concave profile), and *iii*) cosine function (convex profile). In the interval $(0, L/2)$ they are defined by equations:

$$W(t) = W_0 - (W_0 - W_{\min})2t \quad (10)$$

$$W(t) = W_0 - (W_0 - W_{\min}) \frac{1 - e^{-2t}}{1 - e^{-1}} \quad (11)$$

$$W(t) = W_0 - \frac{1}{2} (W_0 - W_{\min}) [1 - \cos(2\pi t)] \quad (12)$$

where $t = z/L$.

In calculations of the propagation length for N -fold images based on Eq. (9) it has been assumed that the ratio of the effective widths of the sections is the same as the ratio of geometrical widths. In the case of symmetrical section the equation:

$$\int_0^1 \frac{W_0^2}{W^2(t)} dt = 2 \int_0^{1/2} \frac{W_0^2}{W^2(t)} dt \quad (13)$$

is satisfied.

Substituting Eqs. (10)–(12) and calculating the integrals we get the equations determining the propagation length for N -fold images, in which $\sigma = W_{\min}/W_0$. We have respectively for linear profile:

$$\frac{\frac{L_N}{L_N^0}}{L_N} = \sigma \quad (14)$$

for exponential profile:

$$\frac{L_N}{L_N^0} = \frac{\sigma e - 1}{e - 1} \left[1 - \frac{1}{\sigma} + \frac{e - 1}{\sigma e - 1} (1 + \ln \sigma) \right]^{-1} \quad (15)$$

for cosine profile:

$$\frac{L_N}{L_N^0} = \frac{2\sigma^{2/3}}{1 + \sigma} \quad (16)$$

Calculated functions are compared in the analyzed range of changes of the width of MMI section in Fig. 7. The functions expressed by Eqs. (15) and (16) are nearly linear. The relative change of the length of propagation is in the case of the linear profile equal to the relative changes of the section widths. A similar dependence is to be observed in the case of the cosine profile. In the case of the MMI section described by the exponential function the rate of changes of the relative length of propagation is somewhat higher.

4. Characteristics of the splitter 1×2 with a varying geometry

In order to verify the results obtained and to check their application in gradient MMI structures made by K–Na ion exchange, the characteristics of the behavior of symmetrical splitter 1×2, presented in Fig. 6, have been simulated making use of the finite difference beam propagation method (FD BPM). For each change of the geometry of the MMI section the optimal length of the splitter was determined, ensuring the self-imaging 1×2 of the input field.

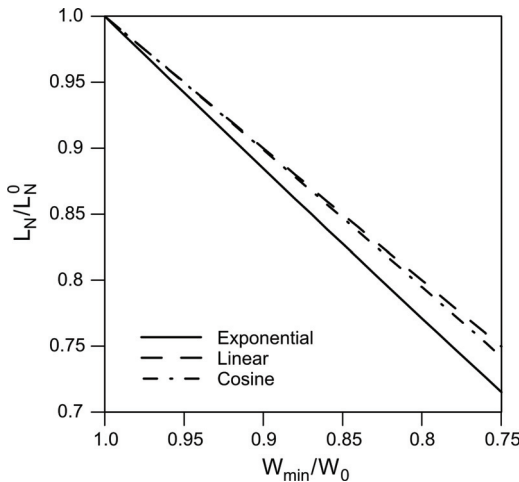


Fig. 7. Dependence of the relative change of the propagation lengths for N -fold images on the relative change of the width of contraction, calculated using Eqs. (14)–(16).

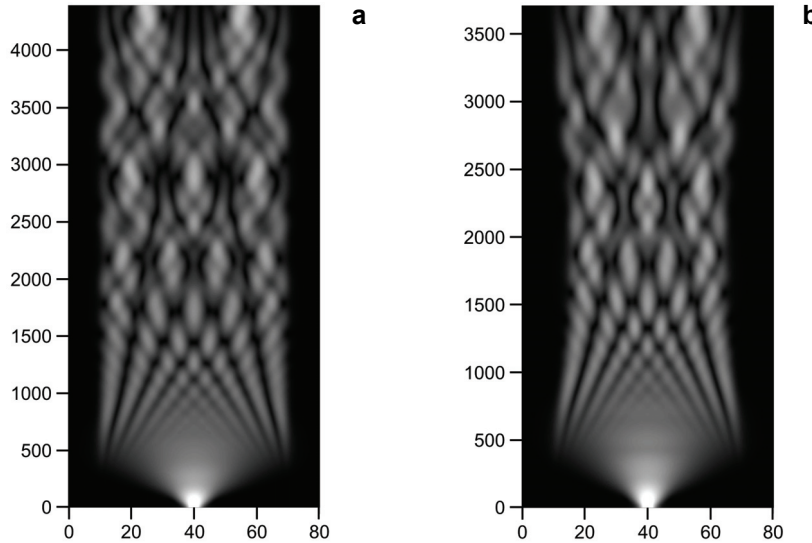


Fig. 8. Amplitude distribution as a function of the propagation length in the straight section of the window width of $W_0 = 60 \mu\text{m}$ (a), the curved structure according to Eq. (12), at a minimum width of $W_{\min} = 50 \mu\text{m}$ (b).

The calculations concerned three different widths of the window W_0 amounting to 40, 50 and 60 μm , as well as various widths W_{\min} . In the function of the shape of splitter defined by Eqs. (10)–(12), these widths were changed within the range of $W_0 - 0.75 W_0$. For each step of propagation the non-linear diffusion Eq. (4) through the window $W(z)$ was solved, and a two-dimensional profile of the refractive index distribution was determined.

Exemples of the results of simulations have been gathered in Fig. 8, where the distribution of the amplitude in straight section of the window width of $W_0 = 60 \mu\text{m}$ is compared with the amplitude in the curved structure according to Eq. (12) for the minimum width $W_{\min} = 50 \mu\text{m}$.

Based on the analysis of interference patterns the length $L_{3\text{dB}}$ of the MMI section was determined in which two-fold images were formed, as well as excess losses α , defined by the equation:

$$\alpha = -10 \log \frac{A_1^2 + A_2^2}{A_0^2} \quad (17)$$

where A_0, A_1, A_2 denote the amplitudes in single-mode input and output waveguides, respectively.

Figures 9a–9c illustrates the dependence of $L_{3\text{dB}}$ on W_{\min} concerning MMI section with initials width equal to 40 μm , 50 μm and 60 μm , respectively, the geometry of which is defined by the functions (10)–(12). Dependences in Fig. 9a for linear and cosine functions run very close to each other. The values of excess losses of the splitter

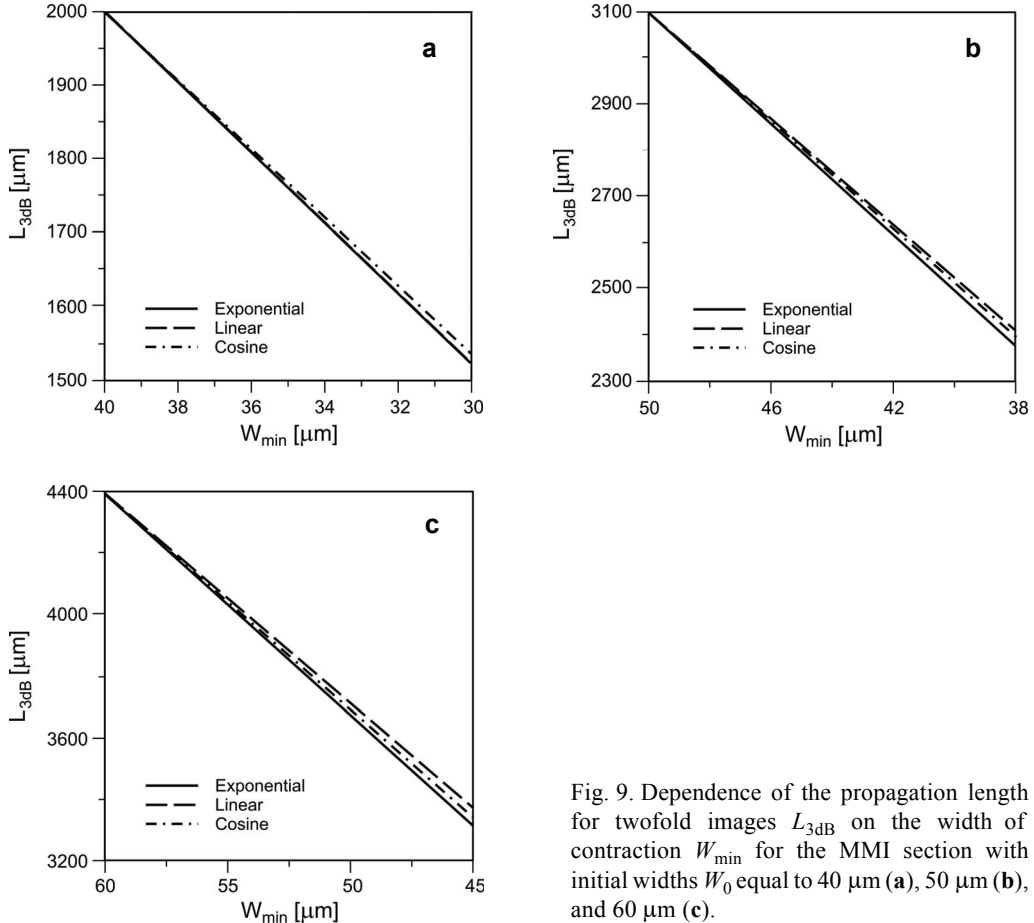


Fig. 9. Dependence of the propagation length for twofold images L_{3dB} on the width of contraction W_{min} for the MMI section with initial widths W_0 equal to 40 μm (a), 50 μm (b), and 60 μm (c).

1×2 , corresponding to these sections, are presented in Fig. 10. Analyzing the characteristics we see that the greatest shortening of the propagation length L_{3dB} occurs in the concave profile, defined by the exponential function, where also the least excess losses in the splitter can be observed. As far as the linear shape from Eq. (10) and cosine shape from Eq. (12) are concerned, the rates of propagation length changes are nearly the same, whereas the convex profile is characterized by considerably higher excess losses, achieving in the case of minimum widths W_{min} values exceeding 3 dB.

The rate of changes of propagation length L_{3dB} depends only slightly on the width of the section, as can be seen in Fig. 11a, which demonstrates the dependence of relative changes of L_{3dB} on the relative changes of the MMI section width in the case of the exponential profile. The initial width, however, affects the quantity of excess losses. The characteristics of excess losses as a function of relative changes in the width of the MMI section for the exponential profile are given in Fig. 11b. The largest differences are to be observed in the case of straight section. The excess losses grow with the curving increasing and become nearly the same.

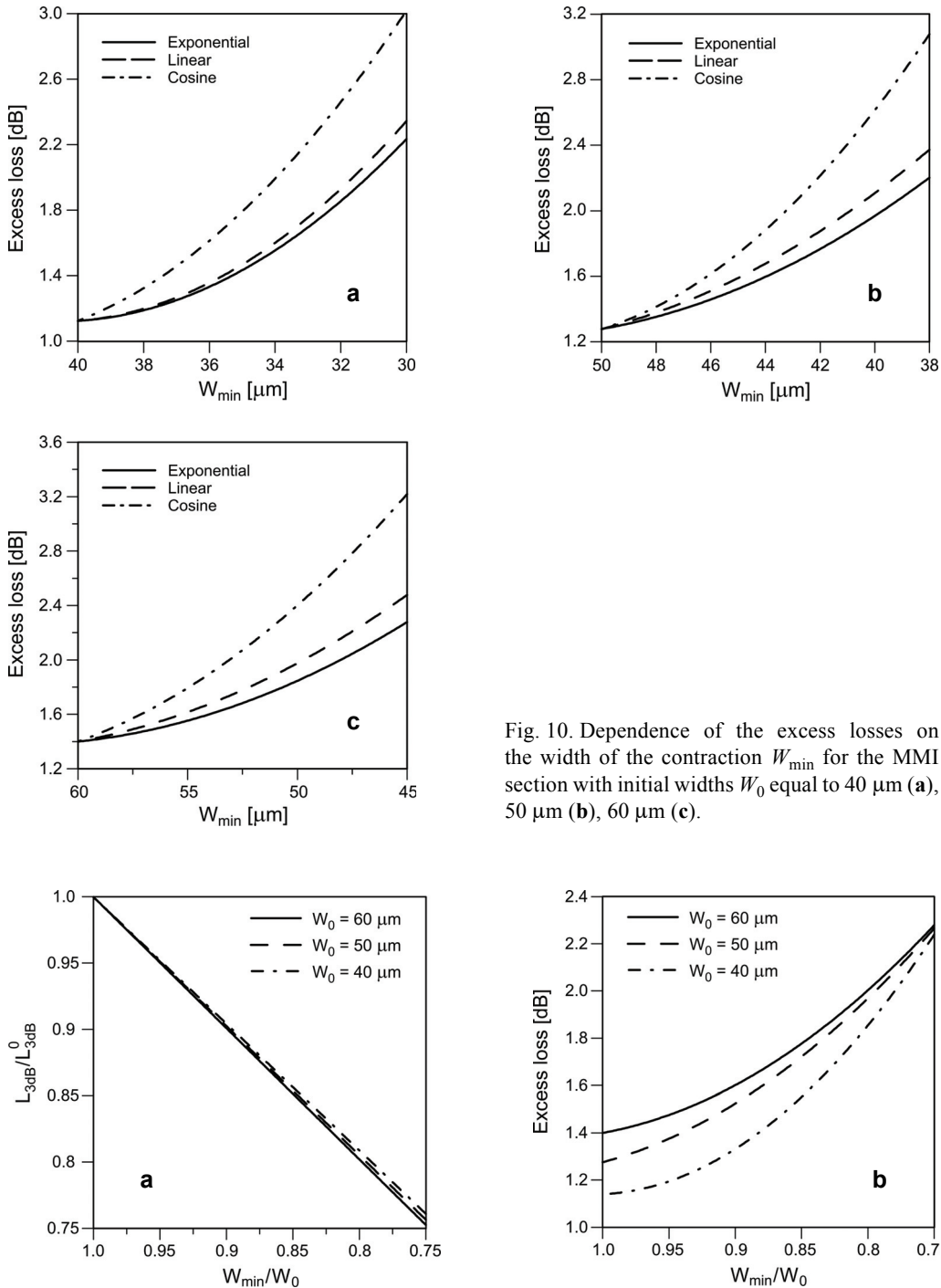


Fig. 10. Dependence of the excess losses on the width of the contraction W_{\min} for the MMI section with initial widths W_0 equal to 40 μm (a), 50 μm (b), 60 μm (c).

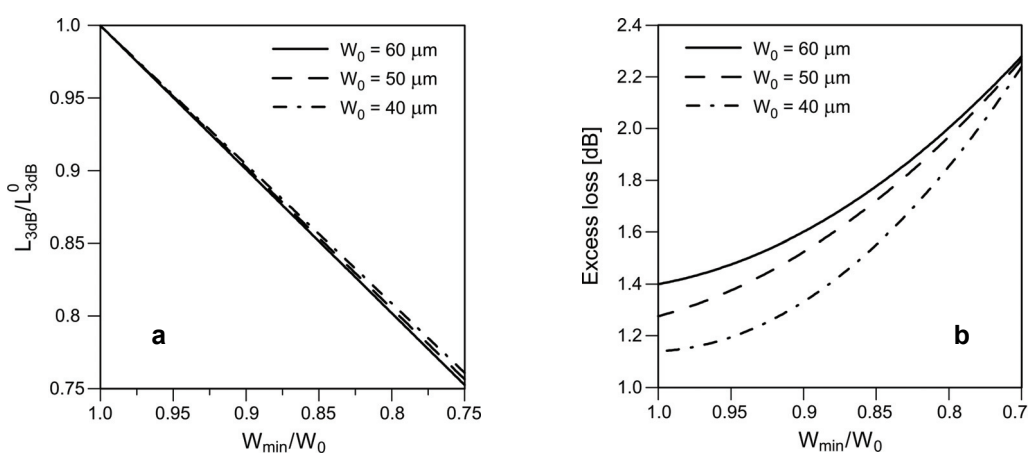


Fig. 11. Dependence of relative changes of the propagation length L_{3dB} (a) and excess losses (b) on relative changes of the MMI section widths for exponential profile.

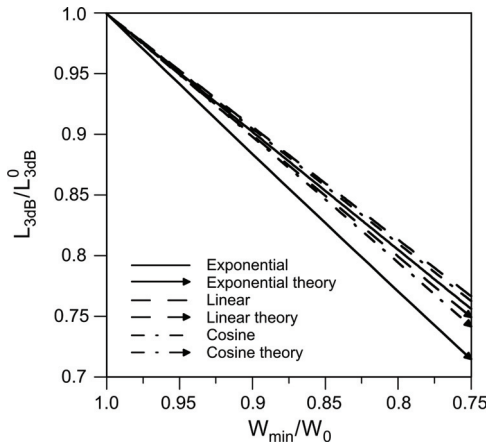


Fig. 12. Dependences of relative changes of the propagation lengths L_{3dB} on the relative changes of the width of the section concerning the analyzed shapes of the MMI section and the initial width $W_0 = 50 \mu\text{m}$. Characteristics are compared with theoretical results on the basis of Eqs. (14)–(16).

In order to compare the results of numerical simulations with theoretical results presented in Fig. 7, we present in Fig. 12 the dependences of relative changes of the propagation length L_{3dB} on relative changes of the width of the section concerning the analyzed shapes of the MMI section and the initial width $W_0 = 50 \mu\text{m}$. The progress of characteristics for the linear and the cosine profiles is in both cases very similar, and the rate of changes of propagation length L_{3dB} is only slightly less in numerical simulations. Larger discrepancies can be observed for the exponential shape, although even in this case the differences in the courses of both functions do not exceed 7%.

5. Restrictions concerning the length of the splitter

The minimum value of the width of section $W_{\min} = 0.75 W_0$, assumed in this paper, results from the changes of interference pattern at the output of the MMI structure, observed in numerical simulations. As soon as a certain value of the contraction has been exceeded, a gradual degradation of the image of the two-fold input field becomes evident. Two-fold images begin to shift towards the axis of symmetry of the structure, and in the centre an additional maximum occurs, whose amplitude grows with the decrease of the width W_{\min} .

The effects observed are presented in Fig. 13. The first image illustrates the distribution of amplitude at the output of the straight section of a width of $W_0 = 60 \mu\text{m}$. The other distributions present interference pattern at the output of the curved MMI structure with an exponential profile. Each subsequent one of them corresponds to a change of the contraction of the section by $5 \mu\text{m}$. For the arbitrary minimum value of the contraction W_{\min} assumed in the paper, amounting in this case to $45 \mu\text{m}$, the amplitude of additional maximum in the centre of the interference pattern does not exceed 20% of the value of the amplitudes of twofold images.

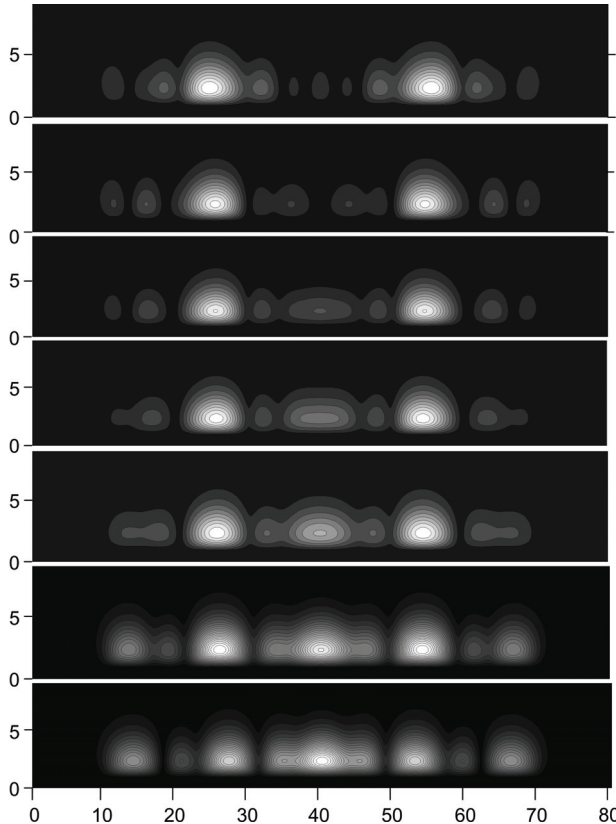


Fig. 13. Distribution of the amplitudes at the output of splitters with an exponential profile, starting with the straight section of the width $W_0 = 60 \mu\text{m}$, and successive ones corresponding to respective changes of contraction by $5 \mu\text{m}$ each.

The interference patterns at the output of the section are similar in all the other analyzed widths W_0 . The observed degradation of twofold images of the input field results most probably from the coupling of modes in curved MMI sections, connected with too fast a change of the width of the section. This effect restricts the possibilities of shortening the length of the coupler $1 \times N$ based on gradient curved MMI structures.

6. Conclusions

The results presented in this paper indicate the possibilities of assessing self-imaging phenomena in gradient MMI structures made by $\text{K}^+ - \text{Na}^+$ ion exchange based on the characteristics of equivalent step-index waveguides. This permits one to determine the propagation lengths for N -fold images in curved gradient MMI structures, making use of relations concerning curved step-index waveguides.

The effects of self-imaging were analyzed in curved MMI structures differing in the type of their curvatures – the linear structure, the concave structure defined by

an exponential function and the convex structure, connected with a cosine function. The relations derived characterizing a relative shortening of the propagation length for N -fold images have been confirmed by numerical simulations applying the BPM method, concerning the operating characteristics of a symmetrically excited gradient splitter 1×2 . The largest shortening of the length of the splitter was achieved in the case of the concave profile defined by the exponential function, where also the least excess losses were observed.

While observing in numerical simulations the changes of interference pattern at the output of the MMI structure, it has been found that after some value of the contraction has been exceeded, the twofold image of the input field gradually degrades. This effect restricts the possibilities of shortening the length of the coupler $1 \times N$, based on curved MMI structures of gradient waveguides.

References

- [1] BACHMANN M., BESSE P.A., MELCHIOR H., *General self-imaging properties in $N \times N$ multimode interference couplers including phase relations*, Applied Optics **33**(18), 1994, pp. 3905–3911.
- [2] SOLDANO L.B., PENNINGS E.C.M., *Optical multi-mode interference devices based on self-imaging: principles and applications*, Journal of Lightwave Technology **13**(4), 1995, pp. 615–627.
- [3] BŁAHUT M., OPIŁSKI A., *Multimode interference structures – new way of a passive elements technology for photonics*, Opto-Electronics Review **9**, 2001, pp. 293–300.
- [4] BŁAHUT M., KARASIŃSKI P., KASPRZAK D., ROGOZIŃSKI R., *Visualization method of modal interference in multimode interference structures*, Optics Communications **214**(1–6), 2003, pp. 47–53.
- [5] BŁAHUT M., KASPRZAK D., *Investigations of multimode interference structures made by ion exchange in glass*, Optica Applicata **33**(4), 2003, pp. 613–626.
- [6] BŁAHUT M., KASPRZAK D., *Multimode interference structures – properties and applications*, Optica Applicata **34**(4), 2004, pp. 573–587.
- [7] KASPRZAK D., BŁAHUT M., *Polarization effects in gradient index MMI structures made by $K^+ \leftrightarrow Na^+$ ion exchange*, Proceedings of the 14th European Conference on Integrated Optics ECIO 2007, April 25–27, 2007, Copenhagen, Denmark, p. THG15.
- [8] KASPRZAK D., BŁAHUT M., MACIAK E., *Application of multimode interference effects in gradient waveguides produced by ion exchange in glass*, Journal de Physique IV, 2008, pp. 113–116.
- [9] LEVY D.S., SCARMOZZINO R., OSGOOD R.M., *Length reduction of tapered MMI devices*, IEEE Photonics Technology Letters **10**(6), 1998, pp. 830–832.
- [10] HUNG-CHIH LU, WAY-SEEN WANG, *Analysis of multimode interference coupler with a width of arbitrary-exponent binomial function*, Journal of Lightwave Technology **25**(9), 2007, pp. 2874–2878.
- [11] LATUNDE-DADA K.A., PAYNE F.P., *Theory and design of adiabatically tapered multimode interference couplers*, Journal of Lightwave Technology **25**(3), 2007, pp. 834–839.
- [12] SAHU P.P., *Compact multimode interference coupler with tapered waveguide geometry*, Optics Communications **277**(2), 2007, pp. 295–301.

*Received December 29, 2008
in revised form March 6, 2009*